

Beam lifetimes and ionization cross sections of U^{28+}

G. Weber,^{1,2,*} C. Omet,¹ R. D. DuBois,³ O. de Lucio,⁴ Th. Stöhlker,^{1,2} C. Brandau,¹ A. Gumberidze,¹ S. Hagmann,¹ S. Hess,^{1,6} C. Kozhuharov,¹ R. Reuschl,^{1,5} P. Spiller,¹ U. Spillmann,¹ M. Steck,¹ M. Thomason,³ and S. Trotsenko¹

¹GSI Helmholtzzentrum für Schwerionenforschung GmbH, 64291 Darmstadt, Germany

²Physikalisches Institut, Universität Heidelberg, 69120 Heidelberg, Germany

³University of Missouri-Rolla, Rolla, Missouri 65409, USA

⁴Instituto de Física, Universidad Nacional Autónoma de México, Apartado Postal 20-364, 01000, México DF, Mexico

⁵Institut des NanoSciences de Paris, CNRS, Université Pierre et Marie Curie-Paris 6, 75015 Paris, France

⁶Institut für Kernphysik, Universität Frankfurt, 60325 Frankfurt, Germany

(Received 15 January 2009; published 31 August 2009; corrected 21 September 2009)

Beam lifetimes of stored U^{28+} ions with energies between 10 and 180 MeV/u were measured in the heavy ion synchrotron SIS18 and in the experimental storage ring (ESR) of the GSI accelerator facility. By using the internal gas jet target of the ESR, it was possible to obtain projectile ionization cross sections for collisions with H_2 and N_2 from the lifetime data. The experimental cross sections are compared to theoretical data predicted by the n -body classical-trajectory Monte Carlo (CTMC) method of Olson *et al.* and to calculations of Shevelko *et al.* using the LOSS-R code. In addition, both theoretical approaches are probed by using the resulting cross sections as input parameters for the STRAHSIM code, which models the beam losses and, consequently, the lifetimes in the heavy ion synchrotron SIS18. Both the cross section measurement and the SIS18 lifetime study indicate that the LOSS-R code cross sections are in better agreement with the experimental results than the n -body CTMC calculations.

DOI: 10.1103/PhysRevSTAB.12.084201

PACS numbers: 34.50.Bw

I. INTRODUCTION

The charge exchange processes occurring in energetic ion-atom collisions play a decisive role in many applications, such as ion beam transport in accelerators, beam lines, and storage rings [1,2], as well as the ion-driven inertial fusion [3,4]. There, interactions between the ions and the constituents of the residual gas can lead to a change of the charge state of the projectiles. In the presence of dispersive ion optical elements, the trajectories of up- or down-charged ions are not matching the one of the reference charge state, resulting in a successive defocusing or even loss of the ion beam. Moreover, projectiles hitting the walls of the beam lines give rise to several unwanted effects, such as increased radiation levels, damaging of sensitive instruments, and degrading of the vacuum conditions [5]. The latter process, caused by ion-induced desorption, can even end up in an avalanche process, leading to a rapid loss of the complete beam. Therefore, exact knowledge of the charge changing cross sections is of crucial importance for the planning of experiments in existing accelerators and storage rings as well as for the design of new facilities.

Future experiments intended at the new Facility for Antiproton and Ion Research (FAIR) facilities require intense beams of heavy ions [6]. In order to reach the highest beam intensities, while minimizing the limitations induced by space charge, the use of low-charged, many-electron ions, e.g. the accumulation of 5×10^{11} U^{28+} ions in the

planned synchrotron SIS100, is intended. The so-called booster operation will use the existing heavy ion synchrotron SIS18 of the GSI facility as an injector for the SIS100. It has to deliver 1.25×10^{11} U^{28+} ions at a repetition rate of 2.6 Hz. So far, the maximum extracted number of particles for this ion species is 8×10^9 due to dynamical vacuum effects as described above [7].

In the relevant energy region ranging from a few MeV/u to a few GeV/u, the dominant beam loss process of many-electron ions, where the number of bound electrons is far above the equilibrium charge state, is projectile ionization, sometimes also referred to as stripping or electron loss. While the theoretical description of ionization of few-electron ions, such as H-like and He-like systems, leads to reliable results within a large range of collision energies and atomic numbers Z , calculations for many-electron systems are still a challenging task [8,9]. To benchmark recent theoretical approaches, experimental data is needed. Previous measurements of the ionization cross sections of many-electron, low-charged ions mainly covered the energy region below 10 MeV/u [10–15]. However, a recent beam lifetime measurement using U^{28+} ions in the experimental storage ring (ESR) extended the energy range up to 50 MeV/u [16].

In this work, we report on ionization cross sections obtained from the recent lifetime experiment. The experimental data are compared to n -body classical-trajectory Monte Carlo (n CTMC) calculations by Olson *et al.* [13,17], and the relativistic Born approximation based LOSS-R code of Shevelko *et al.* [18,19]. In addition, experimental lifetime data from the SIS18 are presented and

*g.weber@gsi.de

compared to STRAHSIM [20] calculations based on the cross sections of both theoretical approaches.

II. EXPERIMENT AND RESULTS

At the GSI accelerator facility, U^{28+} ions were preaccelerated in the linear accelerator UNILAC and subsequently injected into the heavy ion synchrotron SIS18 with an energy of 7.1 MeV/u. The SIS18 was used to accelerate the ions which were then either stored at a constant velocity in the SIS18 or injected into the heavy ion storage ring ESR. The magnetic rigidity of the SIS18 is 18 Tm and allows storing U^{28+} beams with energies up to approximately 200 MeV/u, whereas the ESR is limited to 10 Tm, which corresponds to a maximum energy of approximately 50 MeV/u. Consequently, ions with 10, 20, 40, and 50 MeV/u, respectively, were injected into the ESR, while the same energies and, in addition, 80, 120, and 180 MeV/u, respectively, were used in the SIS18. In order to reduce the contribution of dynamical vacuum effects to the beam lifetime, low beam intensities of the order of 1×10^8 particles were injected into the SIS18. After injection into the ESR, electron cooling was applied, resulting in a strongly reduced emittance and a typical beam diameter of 2 mm.

The loss rate of the stored ions was obtained by measuring the ion current as a function of time using the beam current transformers in both rings. As can be seen in Fig. 1, the beam intensity $I(t)$ follows an exponential decay law,

$$I(t) = I(0) \cdot \exp(-\lambda \cdot t), \quad (1)$$

with t denoting the time and λ the decay constant. The latter is related to the beam lifetime τ by $\lambda = 1/\tau$. Therefore, λ , and consequently τ , can be obtained by a

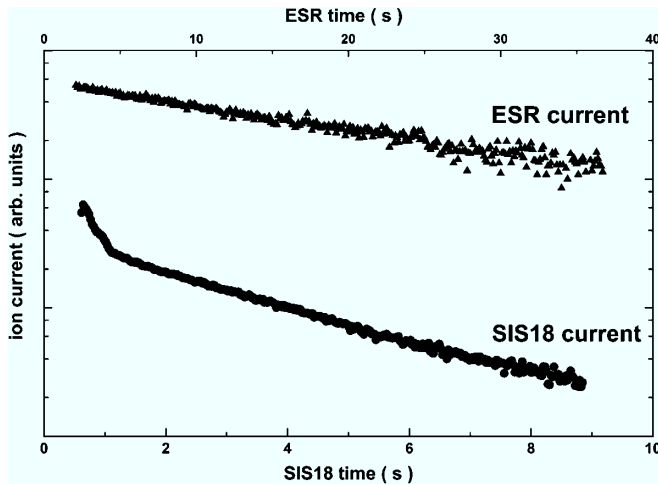


FIG. 1. Logarithmic plot of the U^{28+} ion current versus time at 10 MeV/u in the SIS18 synchrotron (lower curve) and the ESR storage ring (upper curve). The fast decay near the starting point of the SIS18 curve is due to injection losses and acceleration effects.

least-squares adjustment of Eq. (1) to the slope of the ion current. For many-electron ions interacting with the residual gas components at energies above a few MeV/u, projectile ionization is the main beam loss process. Thus, the beam lifetimes are determined by

$$\tau = (\rho \sigma v f)^{-1}, \quad (2)$$

where σ is the weighted mean of the individual ionization cross sections for the different residual gas components, ρ is the gas density, v is the projectile velocity, and f is the fractional length of the interaction region compared to the full cycle length, e.g. $f = 1$ in the case of interactions with the residual gas covering the whole ring. The beam lifetimes obtained in the SIS18 are denoted in Table I, while the ESR lifetimes can be found in [16].

The measured beam lifetimes in the ESR had to be corrected for beam losses due to recombination events in the electron cooler region. Therefore, the lifetime for different electron currents was measured and then extrapolated to zero current conditions. The lifetimes for the SIS18 are roughly a factor 10 shorter than for the ESR. This is due to the different residual gas compositions and their associated partial pressures, which are presented in Table II.

TABLE I. Measured lifetimes of U^{28+} beams at various energies in the SIS18 synchrotron. The errors account for a systematic uncertainty due to the low precision of the beam current transformer at low beam intensities.

Energy [MeV/u]	Beam lifetime [s]
	SIS18
10	3.14 ± 0.47
20	4.27 ± 0.64
40	5.31 ± 0.80
50	5.50 ± 0.83
80	6.27 ± 0.94
120	7.17 ± 1.08
180	8.16 ± 1.22

TABLE II. Estimated residual gas composition in the SIS18 synchrotron and the ESR storage ring. The values should be considered as a rough estimate. Deviations from 100% are due to round-off errors.

Constituent	Residual gas composition	
	SIS18	ESR
H ₂	76%	83%
He	3%	...
CH ₄	12%	5%
H ₂ O	5%	10%
CO/N ₂	3%	...
CO ₂	...	1%
O ₂	0.5%	...
Ar	1%	1%

The data arise from an averaging over local residual gas pressure measurements at different positions inside the ring. The total base pressure in the SIS18 is in the order of 1×10^{-10} mbar and in the ESR is 2×10^{-11} mbar, respectively. As vacuum conditions may differ significantly on the scale of a few meters, these values should be considered as a rough estimate.

As the residual gas contains different constituents, the measured beam lifetime leads to an effective cross section for a particular gas composition, and it is not possible to extract ionization cross sections for an individual component. Therefore, the gas target of the ESR was used for dedicated cross section measurements. With the use of the supersonic gas jet target, it was possible to generate target densities of the order of 10^{12} particles/cm³ with a target diameter of approximately 5 mm [21–23]. H₂ and N₂, often used as reference components to model certain residual gas compositions, served as target gases. The measurement procedure was as follows: After injection into the ESR, the U²⁸⁺ beam was cooled for a few seconds, then the gas target was switched on by opening a fast valve, resulting in a strongly reduced beam lifetime. By scanning the ion beam axially across the target region and measuring the lifetime, the best target-beam overlap position, identified as that corresponding to the shortest lifetime, was found. Once maximum overlap was established, the beam lifetime was measured several times for each beam energy; see [16] for details. In order to extract the lifetime due to interactions with the gas target only, the previously measured contributions of the residual gas and the electron cooler were subtracted. Finally, target dependent ionization cross sections were obtained by solving Eqs. (1) and (2) combined with the gas target density calibration information obtained from [21].

In Fig. 2 the ionization cross sections per target atom for U²⁸⁺ colliding with H and N atoms obtained in this work, as well as previous results from Franzke *et al.* [10] and Olson *et al.* [13], are compared to theoretical predictions by the *n*CTMC method of Olson *et al.* [13] and recent results of the LOSS-R code developed by Shevelko *et al.* [24]. Thereby, the influence of the molecular binding of H₂ and N₂ on the cross sections is neglected. The error bars are due to an estimated uncertainty of 25% in the determination of the target density obtained by measuring the gas load in the dump area of the target device. In the case of the H₂ target, the beam lifetime was long enough such that the analysis could be performed using the part of the ion current decay curve long after the target had already reached its final density (about a few tenths of a second). However, due to the larger cross section resulting in a much more rapid decrease in beam intensity for the N₂ target, the lifetimes had to be extracted using data beginning only a few tenths of a second after the gas target valve was opened. Therefore, it is possible that this could result in the N₂ target density being overestimated, which would

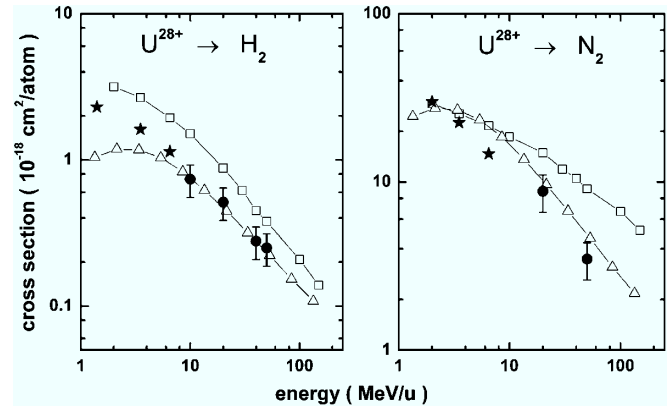


FIG. 2. Experimental cross sections per target atom in comparison to calculations performed by Olson *et al.* (open squares) [13] and Shevelko *et al.* (open triangles) [24]. The experimental data points obtained in this work are denoted by full circles, while data from previous measurements by Franzke *et al.* [10] and Olson *et al.* [13] are denoted by full stars.

lead to an underestimation of the N cross sections. Unfortunately, the use of lower target densities resulting in longer beam lifetimes was not possible due to technical restrictions of the target apparatus.

As can be seen in Fig. 2, for the H cross sections both theoretical approaches and the experimental data all exhibit a very similar energy dependence in the high energy regime, while the absolute values for the two theoretical calculations differ approximately by a factor of 2. The experimental data lie closer to the calculations by Shevelko. Taking into account the limited accuracy of the theoretical approaches, both calculations as well as the experimental results are in agreement with each other. In the case of N there is a significant deviation in the energy dependence between the two theoretical approaches applied. The decrease of the cross section with increasing energy is significantly faster in the case of the LOSS-R code data. The experimental data also indicate a strong decrease, in disagreement with the one of the *n*CTMC method. This result is quite surprising as classical-trajectory Monte Carlo calculations, such as the *n*CTMC method, are known to provide appropriate results for many applications where many-electron systems are involved. However, the reader should keep in mind that this finding is based on two experimental data points only and that our results may be influenced by the experimental uncertainties described above.

Using the predicted cross sections as input parameters for beam lifetime simulations is another way to benchmark different theoretical approaches. Compared to dedicated cross section measurements, this method has the drawback that cross sections for different residual gas components are averaged to an effective cross section, while the composition, as well as the total pressure of the residual gas, is only roughly known. Nevertheless, a comparison between calculated and measured lifetimes may at least serve as an

indicator for the reliability of predicted cross sections. Moreover, as U^{28+} beam lifetime data is available up to 180 MeV/u, while for that ion species the cross section measurements at the ESR gas target are restricted to energies not higher than 50 MeV/u, theoretical approaches can be probed in a considerably broader energy region.

Within the GSI accelerator group the STRAHLSIM code [20] was developed in order to model charge change induced ion beam losses inside the SIS18 and to predict beam lifetimes for the planned SIS100/300. Besides static vacuum beam lifetime calculations, it has also the ability to simulate dynamic vacuum conditions caused by beam losses and ion stimulated gas desorption. Furthermore, the complete acceleration and storage cycle can be simulated, too. Charge exchange cross sections as a function of beam energy are taken from Olson *et al.* or Shevelko *et al.*, and can account for multiple ionization, too. As input parameters for the simulations, the definition of the acceleration cycle, the equilibrium residual gas pressure, and its constituents can be entered. Other vacuum parameters, such as effective pumping speed, volume, and surface areas, are calculated analytically from the given lattice of the SIS18.

In Fig. 3 the STRAHLSIM beam lifetime results according either to the cross sections provided by the LOSS-R code or to the *n*CTMC results are presented together with the experimental lifetime data obtained in this work, as well as previous measurements from 2001 [25]. As both Olson and Shevelko account for an uncertainty of at least 30% in their cross section predictions, these lines are shown additionally for the simulated lifetimes. The total residual gas

pressure was used as a scaling parameter to let both STRAHLSIM calculations coincide at low energies. The scaling factor was 1.33 for the LOSS-R code cross sections and 1.16 for the *n*CTMC cross sections, respectively, which is within the uncertainty of the residual gas measurement. The quasistatic behavior of the lifetimes based on *n*CTMC calculations is due to their rough $E^{-1/2}$ scaling which leads to a cancellation of decreasing ionization cross section and increasing effective line density with increasing projectile velocity. Both, the experimental lifetimes from this work and the previous measurement are in better agreement with the STRAHLSIM calculations based on the LOSS-R code cross sections than with the predictions of the *n*CTMC method. These results give additional evidence for the outcome of the cross section measurement described above.

Nevertheless one has to note that, according to the residual gas composition in Table II, the SIS18 lifetimes are not sensitive to N cross sections unless the C and O atoms are counted as “N like”. For Xe^{18+} ions at 6 MeV/u colliding with CO, CO₂, O₂, and N₂ targets, it was previously shown that the total projectile ionization cross sections per atom coincide within less than 20% [12]. This procedure leads to an approximate 10 to 1 ratio of H and N atoms in the SIS18. As the cross sections for U^{28+} being ionized by N atoms are roughly an order of magnitude larger than for H atoms, the contributions of both constituents to the effective ionization cross section of the residual gas and, consequently, to the lifetime of the stored U^{28+} beam are comparable.

III. SUMMARY AND CONCLUSIONS

Projectile ionization cross sections of U^{28+} ions colliding with H₂ and N₂ targets were measured in the energy region between 10 and 50 MeV/u at the internal gas jet target of the ESR storage ring. The available experimental data was compared to recent theoretical approaches for the treatment of low-charged, many-electron systems, namely, the *n*CTMC method of Olson *et al.* and the LOSS-R code of Shevelko *et al.* In addition, U^{28+} beam lifetimes were measured in the SIS18 synchrotron up to 180 MeV/u. In combination with the STRAHLSIM code, which models beam losses in the SIS18, this allowed probing the theoretical predictions in an even wider energy range than accessible with the dedicated cross section measurements in the ESR. Both experimental studies are in better agreement with the cross sections provided by the LOSS-R code than with the results of the *n*CTMC method. In particular for the N cross sections, there is a significant deviation between the experimental data and the *n*CTMC predictions at high collision energies. As this finding is unexpected and based on a few data points only, additional measurements will be performed. Future experiments may also significantly benefit from the advantages of the upgrade of the

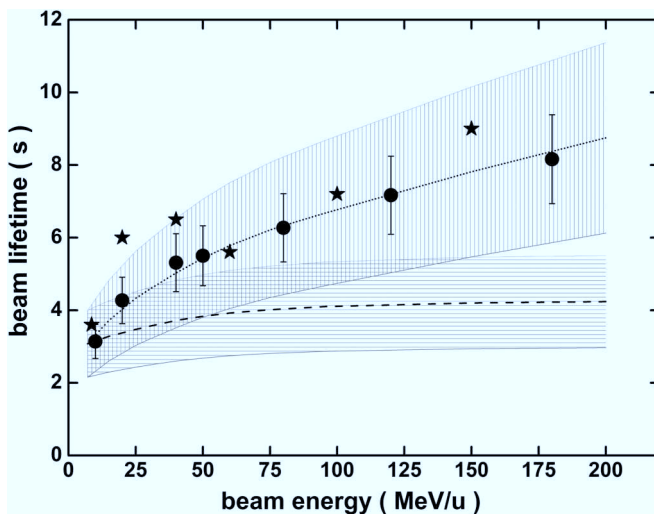


FIG. 3. U^{28+} beam lifetimes in the SIS18 synchrotron plotted versus the beam energy. The experimental data obtained in this work are marked by full circles, while stars denote results from a previous measurement [25]. The STRAHLSIM results together with an error margin of 30% (shaded area) are illustrated by a dotted line (LOSS-R code cross sections) and a dashed line (*n*CTMC cross sections), respectively.

ESR gas jet target apparatus [26], in particular, the wider range of available target densities.

ACKNOWLEDGMENTS

This work was supported in part by the Office of Fusion Energy Research, U.S. Department of Energy. We also would like to thank Ronald E. Olson and Viatcheslav P. Shevelko for the fruitful discussions and continuous theoretical support during this work.

-
- [1] J. Eichler and T. Stöhlker, Phys. Rep. **439**, 1 (2007).
 - [2] V. P. Shevelko, O. Brinzaescu, W. Jacoby, M. Rau, and T. Stöhlker, Hyperfine Interact. **114**, 289 (1998).
 - [3] R. E. Olson, Nucl. Instrum. Methods Phys. Res., Sect. A **464**, 93 (2001).
 - [4] I. D. Kaganovich, E. A. Startsev, and R. C. Davidson, Phys. Rev. A **68**, 022707 (2003).
 - [5] A. W. Molvik *et al.*, Phys. Rev. Lett. **98**, 064801 (2007).
 - [6] FAIR Baseline Technical Report (2006), available online: <http://www.gsi.de/fair/reports/btr.html>.
 - [7] C. Omet, Ph.D. thesis, University of Darmstadt, 2008.
 - [8] I. D. Kaganovich, E. Startsev, and R. C. Davidson, New J. Phys. **8**, 278 (2006).
 - [9] V. P. Shevelko, M. S. Litsarev, M.-Y. Song, H. Tawara, and J.-S. Yoon, J. Phys. B **42**, 065202 (2009).
 - [10] B. Franzke, IEEE Trans. Nucl. Sci. **28**, 2116 (1981).
 - [11] D. Mueller, L. Grisham, I. D. Kaganovich, R. L. Watson, V. Horvat, K. E. Zaharakis, and M. S. Armel, Phys. Plasmas **8**, 1753 (2001).
 - [12] R. L. Watson, Y. Peng, V. Horvat, G. J. Kim, and R. E. Olson, Phys. Rev. A **67**, 022706 (2003).
 - [13] R. E. Olson, R. L. Watson, V. Horvat, A. N. Perumal, Y. Peng, and T. Stöhlker, J. Phys. B **37**, 4539 (2004).
 - [14] R. D. DuBois, Nucl. Instrum. Methods Phys. Res., Sect. B **241**, 87 (2005).
 - [15] M. Kireeff Covo, I. D. Kaganovich, A. Shnidman, A. W. Molvik, and J. L. Vujic, Phys. Rev. A **78**, 032709 (2008).
 - [16] R. D. DuBois *et al.*, Nucl. Instrum. Methods Phys. Res., Sect. B **261**, 230 (2007).
 - [17] R. E. Olson, J. Ullrich, and H. Schmidt-Böcking, Phys. Rev. A **39**, 5572 (1989).
 - [18] V. P. Shevelko, I. Y. Tolstikhina, and T. Stöhlker, Nucl. Instrum. Methods Phys. Res., Sect. B **184**, 295 (2001).
 - [19] I. L. Beigman, I. Y. Tolstikhina, and V. P. Shevelko, Tech. Phys. **53**, 547 (2008).
 - [20] C. Omet, P. Spiller, J. Stadlmann, and D. H. H. Hoffmann, New J. Phys. **8**, 284 (2006).
 - [21] A. Krämer, Ph.D. thesis, University of Frankfurt, 2000.
 - [22] H. Reich, W. Bourgeois, B. Franzke, A. Kritzer, and V. Varentsov, Nucl. Phys. A **626**, 417 (1997).
 - [23] A. Krämer, A. Kritzer, H. Reich, and T. Stöhlker, Nucl. Instrum. Methods Phys. Res., Sect. B **174**, 205 (2001).
 - [24] V. Shevelko (private communication).
 - [25] A. Krämer *et al.*, in *Proceedings of the 8th European Particle Accelerator Conference, Paris, 2002* (EPS-IGA and CERN, Geneva, 2002).
 - [26] M. Kühnel, N. Petridis, D. F. A. Winters, U. Popp, R. Dörner, T. Stöhlker, and R. E. Grisenti, Nucl. Instrum. Methods Phys. Res., Sect. A **602**, 311 (2009).